Kinetics of Hyperbranched Polystyrenes by Free Radical Polymerization of Photofunctional Inimer

Koji Ishizu,* Yoshihiro Ohta, and Susumu Kawauchi

Department of Organic Materials and Macromolecules, International Research Center of Polymer Science, Tokyo Institute of Technology, 2-12-1, Ookayama, Meguro-ku, Tokyo 152-8552, Japan

Received December 4, 2001
Revised Manuscript Received February 20, 2002

Introduction

Highly branched topologies have become a major research interest in polymer science. The synthesis of hyperbranched polymers has been explored to develop dendrimers in a single, one-pot reaction. Recent advances in living polymerization have allowed facile preparation of hyperbranched polymers. The self-condensing vinyl polymerization process first demonstrated using a living cationic polymerization[1] was later expanded to 2,2,6,6-tetramethylpiperidinyloxy (TEMPO)-mediated living radical[2] and group-transfer polymerization process.[3,4] Atom transfer radical polymerization (ATRP) of *p*-chloromethylstyrene (CMS) similarly provided hyperbranched polymers.[5,6] Moreover, we presented a novel route to hyperbranched polystyrenes (PS) from *N*,*N*-(diethylamino)dithiocarbamoylmethylstyrene (DTCS: **1**) as an inimer by one-pot photopolymerization.[7] ^{1}H nuclear magnetic resonance (NMR) spectra of such hyperbranched polymers confirmed the presence of the hyperbranched structure, and the number of active sites was equal to the number of monomer units. Branched PSs were also prepared by free radical copolymerization of **1** with styrene under UV irradiation.[8] Two monomers (**1** and styrene) showed equal reactivity toward both propagation species, and the copolymer composition was the same as the comonomer feed. It was found from the dilute-solution properties that hyperbranched homopolymer behaved as hard spheres in a good solvent. To gain insight into the reaction process of such self-addition vinyl polymerization, it is necessary to analyze the kinetics of this reaction.

Recently, Müller and co-workers[9] calculated the molecular parameters of hyperbranched PSs formed by self-condensing vinyl polymerization of CMS inimer with the general structure AB*, where A is a vinyl group and B* is an initiating group. The calculated molecular weight distribution was extremely broad, the polydispersity index being equal to the number-average degree of polymerization. Our photopolymerization system also proceeds with almost similar mechanism described above. That is to say, the chain initiation is the addition of the active B* group to the double bond of another monomer (see Scheme 1). Photolysis of **1** leads to the initiating benzyl radical with a less reactive carbamate (DC) radical that undergoes primary radical termination.[10−12] The dimer **2** formed has two DC active sites and one double bond. Both the initiating B* group and the newly created propagating center, A*, can react with the vinyl group of any other molecule (monomer or polymer) in the same way with rate constant k_A and k_B, respectively. The initial steps up to the formation of trimers **3** are shown in Scheme 1. The addition of a vinyl group to a terminal A* or B* center leads to a linear linkage, whereas the addition of a double bond to a side group B* (**3b**) or an A* center within the polymer (center of **3a**) leads to a branch point. In further polymerization steps, the fraction of branched structures is generated. In this note, we studied the kinetics of hyperbranched PSs by free radical polymerization of photofunctional inimer **1** and the degree of branching (DB). We also demonstrated that density functional theory calculations provide a reliable and quantitative prediction of experimentally observed trends in C−S bond dissociation energies for several model compounds.

Scheme 1

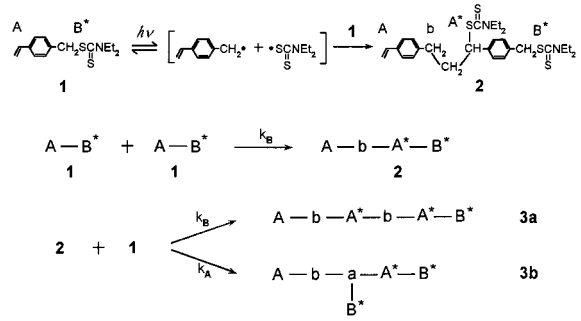

Scheme 2

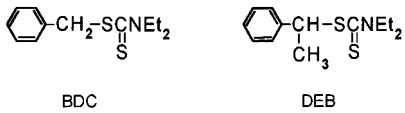

BDC DEB

Experimental Section

Photopolymerization. Inimer DTCS was synthesized by the reaction of CMS (Seimi Chemical Industry) with *N*,*N*-diethyldithiocarbamate sodium salt in acetone. Details concerning the synthesis and purification of DTCS have been given elsewhere.[7] Model compound 1-(*N*,*N*-diethyldithiocarbamyl)ethylbenzene (DEB, see Scheme 2) was also synthesized by a similar reaction using 1-phenyl-1-chloroethane to assign the chemical shift of proton signals in NMR. Photopolymerizations of **1** (50 wt % benzene solution) were carried out varying the irradiation time at 25 °C (system A; 250 W high-pressure mercury lamp). After polymerization, the polymer was recovered by evaporating the solvent. We also carried out the photopolymerization of **1** in the presence of *N*,*N*-tetraethylthiuram disulfide (TD) (0.1 equiv of **1**; system B). TD was used as a chain transfer agent and a source of the DC radical, which participates in primary radical termination.

Characterization. A combination of gel permeation chromatography (GPC) with light scattering (LS) detector is very useful for measuring the weight-average molecular weight ($\bar{M}_w$) and molecular weight distribution ($\bar{M}_w/\bar{M}_n$) of hyperbranched molecules. GPC measurements were carried out with a Tosoh high-speed liquid chromatograph HLC-8120 equipped with a low-angle laser light scattering (LALLS) detector, LS-8 (He−Ne laser with a detection angle of 5°), and refractive index (RI), which was operated with two TSK gel columns, GMH_{XL} and $G2000H_{XL}$, in series using tetrahydrofuran (THF) as the eluent. The conversion was estimated from the vinyl protons (δ 5.26 and 5.74 ppm) of unreacted inimer **1** in the ^{1}H NMR spectrum of each product (500 MHz, JEOL GSX-500 NMR spectrometer in $CDCl_3$). We also discussed the degree of branching (DB) of hyperbranched polymers by the results of NMR spectra.

10.1021/ma012109c CCC: $22.00
Published on Web 03/27/2002

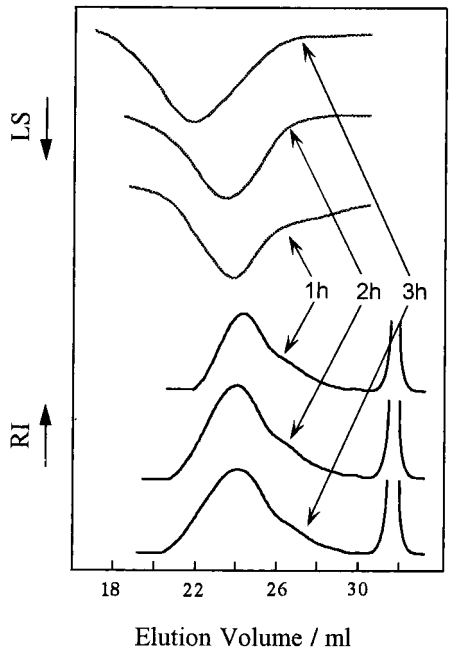

Figure 1. GPC profiles for system B as a function of irradiation times.

Density Functional Theory Calculations. To shed more light on the observed reactivities, we performed density functional theory calculations (B3LYP functional using 6-31G-(d) basis set)[13] for various model compounds [benzyl *N*,*N*-diethyldithiocarbamate (BDC) and DEB **1** and **2**; see Schemes 1 and 2]. These calculations have been conducted for a series of carbamates to establish a correction between structure and C−S homolysis rates. C−S bond energies were calculated assuming a hemolytic bond cleavage corrected with zero-point energy.

Results and Discussion

Photopolymerizations of **1** were carried out varying the irradiation time. In no case were cross-linked or insoluble materials observed. GPC profiles for system A showed a bimodal pattern as mentioned in the previous paper.[7] Typical GPC profiles for system B are shown in Figure 1. Each elution peak at the lowest molecular weight side corresponds to that of unreacted inimer **1**. All the GPC distributions of these products have a unimodal pattern, and the molecular weight distributions are not so broad. The degree of polymerization increases with increasing reaction times. The conversion was estimated from the vinyl protons of unreacted inimer **1** in the ^{1}H NMR spectrum of each product.

To better understand the mechanism of propagation, we performed the first-order time−conversion plots in the systems A and B (Figure 2), where $[M]_0$ is the initial concentration of inimer **1**. Straight lines in the semilogarithmic coordinates indicate first order in monomer. The straight lines also indicate a constant concentration of the active species. It is found from these plots that both systems A and B proceed with living radical mechanism. The slopes of the semilogarithmic anamorphoses, $S = R_p/[M]$ (where $R_p = -d[M]/dt$), were set equal to 0.386 and 0.215 h^{-1} for systems A and B, respectively. The slopes are also possibly relative to the reactive ratios k_A/k_B.[9] According to Figure 3 (mentioned later, plot of $\bar{M}_w$ against conversion), system B might have a lower k_A/k_B value. Higher active radical concentration and higher reactive ratios may cause higher

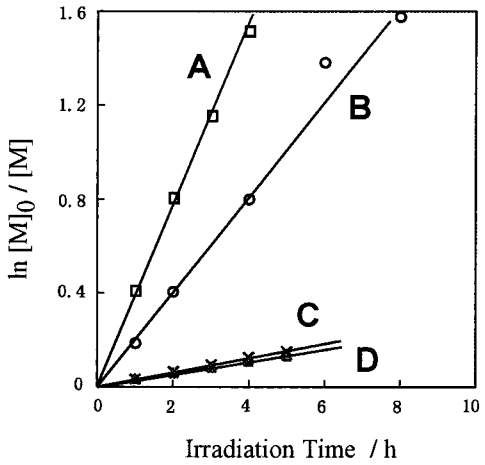

Figure 2. First-order time−conversion plots: curve A, system A, curve B, system B; curve C, polymerization of styrene initiated by DEB; curve D, polymerization of styrene initiated by BDC.

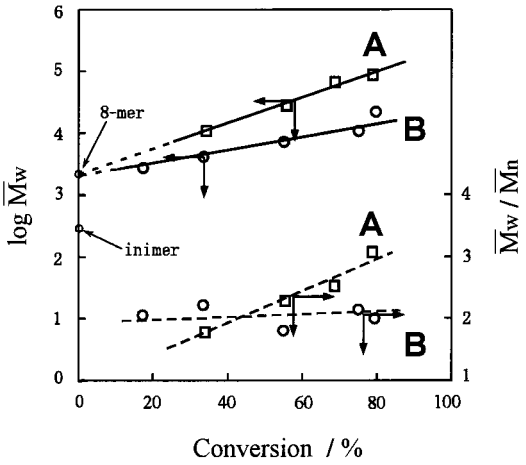

Figure 3. Semilogarithmic plot of weight-average molecular weight ($\bar{M}_w$) or molecular weight distribution ($\bar{M}_w/\bar{M}_n$) against conversion for systems A and B.

slopes in Figure 3. It seemed that system B produced polymers with a very low degree of branching (DB).

Figure 3 shows the semilogarithmic plot of $\bar{M}_w$ or $\bar{M}_w/M_n$ against conversion for systems A and B. The observed values of $\bar{M}_w$ for both systems fit well to the straight line in a semilogarithmic plot. The intercept for systems A and B shows the same value but is larger than expected value. The value of intercept for systems A and B corresponded to the $\bar{M}_w$ of 8-mer. In the case that the reactivity changes with size of the molecules, the molecule size at which the reaction becomes slower should be identical for both systems. This effect is congruent with Fréchet's observation[1] that the condensation occurs faster in the initial stage (less than 10-mer). This may be due to a lower accessibility of reactive centers at the inside of larger branched molecules. On the other hand, the polydispersity for system B is narrower ($\bar{M}_w/\bar{M}_n$ = ca. 2) than that for system A. The addition of TD may move the equilibrium balance between inimer **1** and benzyl/DC radicals (as shown in Scheme 1) to the left side. It was mentioned earlier from Müller's theoretical calculation that the predicted polydispersity increased exponentially with conversion (in the case of $k_A = k_B$ for the formation of hyperbranched polymers). The tendency obtained in system A was very similar to their theoretical results. It was mentioned

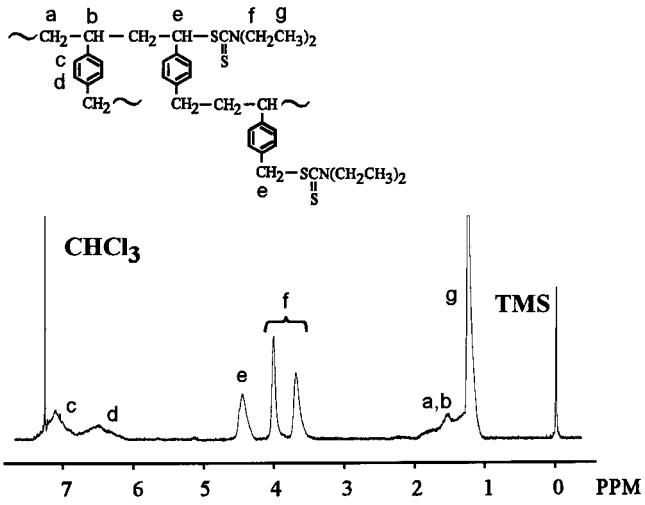

Figure 4. ^{1}H NMR spectrum of hyperbranched polymer produced from system A (irradiation time = 2 h) in $CDCl_3$.

earlier that system B produced hyperbranched polymers with a very low DB. Such DB will be discussed later from ^{1}H NMR spectra of hyperbranched polymers.

Our polymerization system seems to proceed with the competitive reactions between the initiator radical (benzyl radical) and the monomer vinyl radical (secondary phenethyl radical). Both radicals are conjugated with aromatic ring. Otsu and co-workers[14] synthesized various photoiniferters having different structures as shown in Scheme 2, i.e., BDC and DEB. They carried out photopolymerizations of styrene with such iniferters (bulk polymerization at 30 °C, $[BDC]_0 = 7.3 \times 10^{-3}$ mol L^{-1}; $[DEB]_0 = 9.2 \times 10^{-3}$ mol L^{-1}). We performed the first-order time−conversion plots for both polymerizations from the conversion curves published in ref 14 (see in Figure 2; curve C: DEB and curve D: BDC). The observed values fit well on the first-order plots for both polymerizations. Moreover, both slopes of the semilogarithmic anamorphoses are almost same value within experimental error. (The feed concentration of $[BDC]_0$ is somewhat lower compared to $[DEB]_0$.) The kinetics measured are styrene conversion. After the addition of one unit of styrene to either BDC or DEB, the DC radical is attached to the same type of structure group. Therefore, the rate of activation of the dormant chain end will be the same, hence the same rate of polymerization. A more appropriate approach would be to examine the relative rates of disappearance of the two initiators at the early stages of polymerization.

A typical ^{1}H NMR spectrum of hyperbranced PS for system A (irradiation time = 2 h) is shown in Figure 4. This spectrum shows the expected resonances for the aromatic protons of PSs (c and d; δ 6.3−7.3 ppm), the methyl (g; 1.2 ppm), and methylene protons (f; 3.7 and 4.0 ppm) of the DC groups, and the methylene protons adjacent to DC groups (e; 4.5 ppm) and confirms the presence of the hyperbranched structure. The methyne protons −CH− of inimer **1** adjacent to DC groups were overlapped with the signal of methylene protons (e) adjacent to DC groups. (This assignment was achieved using model compound DEB.) In our system, the methylene moieties in which styryl radicals attack the double bond of **1** correspond to branching points. This signal should appear at around 1.9 ppm. So, we cannot discuss quantitatively about DB from ^{1}H NMR spectra because this signal overlaps with PS backbone signals (a and b). However, the integration ratio of signal e to f provides some information as DB. When considering the ideal statistics of chain growth of **1** (perfect dendritic structure), assuming equal reactivity constants for benzyl and styryl radicals ($k_A = k_B$), the integration ratio of signal f to g should be to 3:8. The experimentally observed ratio of 2.8:8 for system indicates an imperfect structure. So, k_B is not equal to k_A for these systems. It seems that macromolecules produced from system A have a higher DB than that produced from system B.

Figure 5 shows the results of C−S bond dissociation energies and bond lengths for several model compounds. Steric factors are important in determining the bond dissociation energies. It might be anticipated that this should be reflected in longer lengths for the breaking C−S bond in the ground state for which steric factors are greatest. The calculations predict that the values of C−S bond lengths do increase in the order DEB > **1** > BDC. In other words, the formation of secondary phenethyl radical is predominant to that of primary benzyl radical. Moad et al.[15] and Kazmaier et al.[16] reported the molecular orbital calculations of alkoxyamine homolysis rates on alkoxyamine-initiated living radical polymerization. Prediction showed a marked dependence on the structure of both the nitroxide and radical components. In the case of secondary and tertiary alkoxyamines, steric factors appeared to be the dominant influence. Bond dissociation tendency observed in our work is very similar to their results. In our calculations, the very slight increase in bond length with decrease in C−S bond dissociation energy for model compounds where the DC fragment is DEB > **1** ∼ BDC (1.863−1.846 Å) is almost well agreement. It is however remarkable that C−S bond dissociation energies of dimer **2** have different trends (see Figure 5). The dimer **2** has two DC active sites. The C−S bond length at A*

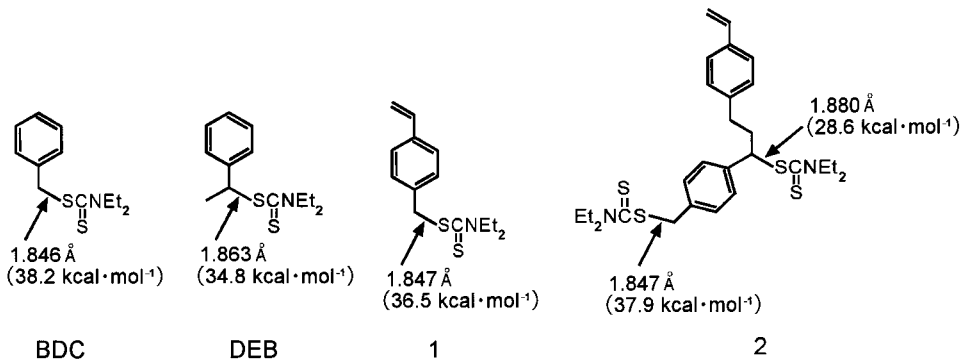

Figure 5. Results of C−S bond dissociation energies and bond lengths for several model compounds calculated assuming a hemolytic bond cleavage at B3L YP/6-31G(d) corrected with zero-point energy.

group is extremely long (1.880 Å). It can be predicted from this result that the propagation rate from A* position will be faster than that from B* position. This effect seems to reflect the experimental results that the additions occurred faster in the initial stage of hyperbranched polymer formation. The density functional theory is better understanding the apparent reactivities. However, the whole process should be taken into account when discussing the kinetics of controlled polymerization.

It is concluded that free radical photopolymerizations of inimer **1** proceed with living radical mechanism such as stepwise polymerization. Hyperbranched macromolecules produced from system A contained much dendritic structures compared to those from system B. Our work thus gives the important suggestion concerning the hyperbranched structure. It is necessary to make clear the DB. This matter will be discussed elsewhere.

Acknowledgment. This work was supported in part by a Grant-in-Aid for Scientific Research, No. 136580927, from the Ministry of Education, Science, Sports and Culture, Japan. The density functional theory calculations were carried out at the Computer Center of Tokyo Institute of Technology and the Computer Center of Institute for Molecular Science, and we thank them for their generous permission to use the SG1 Origin2000 and Compaq Alpha Server GS320 and IBM SP2, respectively. Authors are grateful to Seimi Chemical Industry for providing samples of *p*-chloromethylstyrene.

References and Notes

(1) Fréchet, J. M. J.; Henmi, M.; Gitsov, I.; Aoshima, S.; Leduc, M. R.; Grubbs, R. B. *Science* **1995**, *269*, 1080.

(2) Hawker, C. J.; Fréchet, J. M. J.; Grubbs, R. B.; Dao, J. *J. Am. Chem. Soc.* **1995**, *117*, 10763.

(3) Fréchet, J. M. J.; Aoshima, S. US Patent 5 587 441, 1996.

(4) Fréchet, J. M. J.; Aoshima, S. US Patent 5 587 446, 1996.

(5) Gaynor, S. G.; Edelman, S.; Matyjaszewski, K. *Macromolecules* **1996**, *29*, 1079.

(6) Weimer, M. W.; Fréchet, J. M. J.; Gitsov, I. *J. Polym. Sci., Polym. Chem. Ed.* **1998**, *36*, 955.

(7) Ishizu, K.; Mori, A. *Macromol. Rapid Commun.* **2000**, *21*, 665.

(8) Ishizu, K.; Mori, A. *Polym. Int.* **2001**, *50*, 906.

(9) Müller, A. H. E.; Yan, D.; Wulkov, M. *Macromolecules* **1997**, *30*, 7015.

(10) Otsu, T.; Yoshida, M. *Makromol. Chem. Rapid Commun.* **1982**, *3*, 127.

(11) Otsu, T.; Kuriyama, A. *J. Macromol. Sci., Chem.* **1984**, *A21*, 961.

(12) Otsu, T.; Yamashita, K.; Tsuda, K. *Macromolecules* **1986**, *19*, 287.

(13) Gaussian 98, Revision A. 7: Frisch, M. J.; Trucks, G. W.; Schlegel, H. B.; Scuseria, G. E.; Robb, M. A.; Cheeseman, J. R.; Zakrzewski, V. G.; Montgomery, Jr., J. A.; Stratmann, R. E.; Burant, J. C.; Dapprich, S.; Millam, J. M.; Daniels, A. D.; Kodin, K. N.; Strain, M. C.; Farkas, O.; Ochterski, J.; Petersson, G. A.; Ayala, P. Y.; Cui, Q.; Morokuma, K.; Malick, D. K.; Rabuck, A. D.; Raghavachari, K.; Foreman, J. B.; Cioslowski, J.; Ortize, J. V.; Baboul, A. G.; Stefanov, B. B.; Liu, G.; Liashenko, A.; Piskorz, P.; Komaromi, I.; Gomperts, R.; Martin, R. L.; Fox, D. J.; Keith, T.; Al-Laham, M. A.; Peng, C. Y.; Nanayakkara, A.; Gonzalez, C.; Head-Gordon, M.; Replogle, E. S.; Pople, J. A. Gaussian, Inc., Pittsburgh, PA, 1998.

(14) Otsu, T.; Matsunaga, T.; Doi, T.; Matsumoto, A. *Eur. Polym. J.* **1955**, *31*, 67.

(15) Moad, G.; Rizzardo, E. *Macromolecules* **1995**, *28*, 8722.

(16) Kazmaier, P. M.; Moffat, K. A.; Georges, M. K.; Veregin, R. P. N.; Hamer, G. K. *Macromolecules* **1995**, *28*, 1841.

MA012109C